Volume 7, Number Proof, 2022, 1–

THE COMPUTATION OF WANDERING POINTS ON THE GLOBAL ATTRACTOR BY MEANS OF SYMMETRY-BREAKING PERTURBATIONS

ALEXEY CHESKIDOV, ERIC OLSON, AND BEAU SMITH

Abstract. We start with a traveling-wave solution on the global attractor of the Kuramoto–Sivashinsky equation and we perturb this solution so it is no longer 2π-periodic in space but only 4π-periodic. No matter how small the perturbation, we observe computationally, that, up to a translation in space related to the perturbation, the resulting solution takes essentially the same trajectory before ultimately converging to a fixed point. In our theory, we prove that trajectories which result from small perturbations of a point on the attractor stay close to the attractor; we further prove that the set resulting from a suitable limit of smaller and smaller symmetry-breaking perturbations lies on the global attractor. Moreover, since the symmetric breaking occurs only once, we have found wandering points on the attractor which are nonrecurrent.

1. Introduction

The Kuramoto-Sivashinsky equation was derived in 1974 by George Homsy [14] and Alexander Nepomnyashchii [20] studying liquid film flowing down an inclined plane, in 1976 by Yoshiki Kuramoto and Toshio Tsuzuki [17] studying persistent wave propagation through reaction-diffusion media and in 1977 by Gregory Sivashinsky [23] studying instability in laminar flames. A Painlevé test and the presence of chaotic solutions indicate that no explicit general analytic solutions exist for this equation [7].

The Kuramoto–Sivashinsky equation is given by

$$u_t + uu_x + \mu u_{xx} + \nu u_{xxxx} = 0 \tag{1.1}$$

with initial condition $u(0,x) = u_0(x)$ for $x \in \mathbb{R}$. Here $u(t,x)$ represents, for example, the flame-front velocity, μ is a dimensional constant that represents the heat released by the combustion reaction, and ν represents the heat required to preheat the incoming reactants (see the discussion in the appendix to Chapter 11 in Griffiths and Schiesser [12]). The well-posed nature of (1.1) has been known since Tadmor confirmed it in 1986 [25]. From this point on, this paper will use the abbreviation KSE to refer to (1.1). We shall also write $u(t)$ to stand for the function of x such that $u(t)(x) = u(t,x)$.

Note that if u_0 is periodic in space with period $L > 0$ such that $u_0(x+L) = u_0(x)$, then $u(t,x+L) = u(t,x)$ for all time $t > 0$. We may therefore impose L-periodic boundary conditions on (1.1) and consider the phase space of all L-periodic solutions. Further note that if u_0 has zero average, then $\int_0^L u(t,x)\,dx = 0$ for all

2020 *Mathematics Subject Classification.* 35B41.

Key words and phrases. Global Attractor, Kuramoto–Sivashinsky.

time $t > 0$. Unless otherwise indicated, we shall assume our solutions have zero spatial average.

It is was first shown by Nicolaenko, Scheurer and Temam [21] under the additional assumption $u_0(x) = -u_0(-x)$ that the KSE with L-periodic boundary conditions has a unique global attractor (see also Temam [26], Robinson [22] and references therein). These results were subsequently extended to the case of general L-periodic solutions by Il'yashenko [15] and independently by Collet, Eckmann, Epstein and Stubbe [6]. Gujić [13] found global bounds on the radius of spatial analyticity for a neighborhood about the set of all fixed points while local bounds were used by Arioli and Koch [1] for the rigorous computation of certain fixed points. Rigorous numerics were further used to find periodic orbits by Figueras and de la Llave in [11].

In this paper we use the exponential time integrator derived by Cox and Matthews [8] and refined by Kassam and Trefethen [16] to approximate a periodic solution on the global attractor. We then make a symmetry-breaking perturbation of that periodic solution. After proving our perturbed trajectories remain uniformly near the global attractor, we show in the limit that these trajectories allows us to recover points on the attractor. We then observe numerically that the trajectories resulting from our perturbations all converge to the same fixed point. This allow us to compute wandering points on the global attractor which lie on the unstable manifold of the periodic solution and connect to the fixed point.

Denote the global attractor of the Kuramoto–Sivashinsky equation with L-periodic boundary conditions by $\mathcal{A}_L$. Since an L-periodic function may also be viewed as a $2L$-periodic function, then

$$\mathcal{A}_L \subseteq \mathcal{A}_{2L}.$$

Note that it could happen that $\mathcal{A}_L = \mathcal{A}_{2L}$, for example, when the attractor in both cases reduces to a single point at the origin. On the other hand, it could happen that $\mathcal{A}_L \neq \mathcal{A}_{2L}$ and, moreover, that fixed points and limit cycles in $\mathcal{A}_L$ which are stable become unstable when viewed as part of the larger attractor $\mathcal{A}_{2L}$. In fact, for the choice of parameters given by $L = 2\pi$, $\mu = 0.1$ and $\nu = 0.027$ this is exactly what our numerics suggest.

A point $u_0 \in \mathcal{A}$ is said to be wandering if there is a neighborhood U of u_0 and a positive time T such that $S_t(U) \cap U = \emptyset$ for all $t > T$. Here S_t is the solution semigroup given by $S_t(u_0) = u(t)$ where u is the unique solution to the KSE equation (1.1) with initial condition u_0. Note that any point which is wandering is guaranteed to be nonrecurrent.

Our computational technique to find wandering points on the global attractor of the KSE consists of the following steps:

- Find a periodic orbit on $\mathcal{A}_L$ using long-time computation.
- Perturb that solution so it is no longer L-periodic in space but only $2L$-periodic.
- Make smaller and smaller perturbations.
- Observe all trajectories end at spatial translations of the same fixed point.
- Take a subsequence to obtain a limit trajectory that ends at a single fixed point.
- Observe this final fixed point is $2L$-periodic but not L-periodic.

The theoretical results, stated and proved below as Theorem 2.5 in the context of the KSE and subsequently extended to general dissipative systems as Theorem 3.8 and Theorem 3.9, imply the set of points in phase space resulting from the limit of the trajectories taken as in Theorem 2.8 is guaranteed to lie on $\mathcal{A}_{2L}$. We therefore conclude the points which make up the limit trajectory are nonrecurrent. To further see they are wandering, we note there is a neighborhood about each point consisting of $2L$-periodic functions which are not L periodic and again that all points in those neighborhoods converge to spatial translations of the fixed point found earlier.

To illustrate the idea behind the above technique, we first consider a simple case given by the system of ordinary differential equations

$$x_t = -\tfrac{1}{4}x(x-2)(x+2), \qquad y_t = -y. \tag{1.2}$$

A phase diagram of this system appears as Figure 1. Note that the origin is a saddle point that is stable when solutions are restricted to the y-axis. There are also two stable fixed points at $x = -2$ and $x = 2$ on the x-axis. Therefore, the global attractor of this simple system consists of the points $\mathcal{A} = \big\{\,(x,0) : x \in [-2,2]\,\big\}$. Moreover, the nonrecurrent points are clearly wandering and described by $\mathcal{W} = \big\{\,(x,0) : x \in (-2,0) \cup (0,2)\,\big\}$.

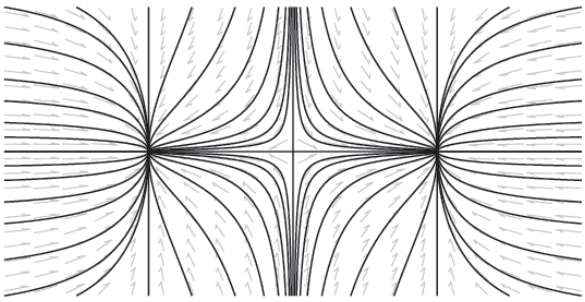

FIGURE 1. Phase portrait of a simple ODE illustrating how symmetry breaking perturbations can find nonrecurrent points on the attractor.

We now describe how the computational steps outlined above can be used to find points in the wandering part $\mathcal{W}$ of the attractor $\mathcal{A}$. In a way analogous to how solutions of the KSE with L-periodic initial conditions remain L-periodic, note that solutions to (1.2) with initial conditions of the form $(0, y_0)$ satisfy $x = 0$ for all time. Let $\mathcal{A}_0$ denote the global attractor in the phase space of all solutions such that $x = 0$. Note that $\mathcal{A}_0 \subseteq \mathcal{A}$. Moreover, $\mathcal{A}_0$ consists of a single fixed point at the origin which is stable subject to the condition that $x = 0$.

In particular, since any trajectory starting with initial condition of the form $(0, y_0)$ eventually arrives at the fixed point $(0, 0)$ in $\mathcal{A}_0$, it is possible to find this point numerically by making a long-term computation subject to the condition $x = 0$. Note that this fixed point point also lies on the global attractor $\mathcal{A}$ of the full system. In the case of the KSE, we take a long time trajectory from an L-periodic initial condition and observe that it converges to a periodic orbit. We then infer this periodic orbit also lies on the global attractor $\mathcal{A}_{2L}$.

Referring back to the simple system, next perturb the point $(0,0)$ by any perturbation of the form (α,β) with $\alpha \neq 0$. By Theorem 2.5, this results in a trajectory that stays close to the global attractor. Moreover, if $\alpha < 0$ the perturbed trajectory now converges to the fixed point $(-2,0)$ on the x-axis and if $\alpha > 0$ it converges to $(2,0)$. By computing trajectories perturbed by smaller and smaller values of α and β and then selecting a subsequence of trajectories that either all tend to $(-2,0)$ or all tend to $(2,0)$, we can identify points in the limit which lie on the attractor. Note that all the points in this limit trajectory (except the beginning and the end) are wandering. In the case of the KSE, rather than two fixed points, the perturbed trajectories will converge to a whole assortment of spatial translations of a single non-L-periodic fixed point in $\mathcal{A}_{2L}$. By again selecting a subsequence we obtain a limit trajectory of wandering points which lie on the attractor $\mathcal{A}_{2L}$.

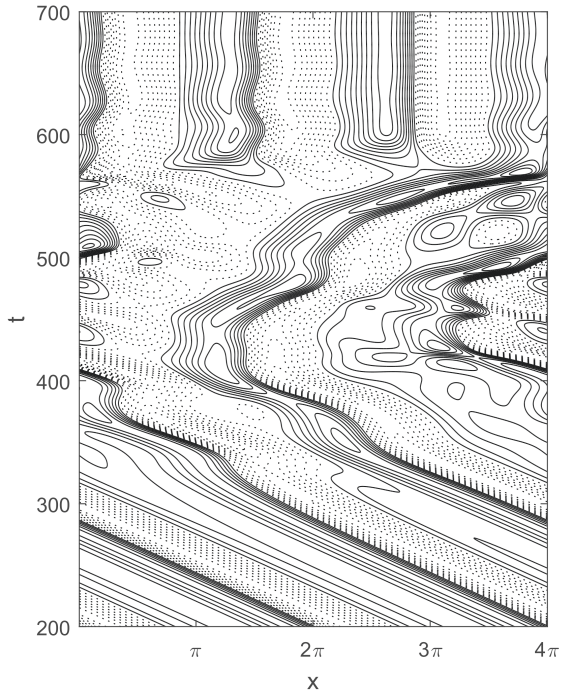

FIGURE 2. Non-recurrent trajectory on the global attractor connecting a 2π-periodic traveling wave to a 4π-periodic fixed point.

To find points on the global attractor of a partial differential equation, a typical numerical approach is to evolve an arbitrary initial condition sufficiently forward in time until the solution is close to the attractor. While it is known for certain choices of the parameters μ and ν that the KSE appears to undergo chaotic motion, for the choice of parameters $\mu = 0.1$ and $\nu = 0.027$, numerically evolving an arbitrary 4π-periodic initial condition forward in time generally leads to a specific fixed point with 6 relative extrema, its various spatial translations or possibly the zero solution. This, of course, assumes the probability is zero that an arbitrary 4π-periodic function

happens also to be 2π-periodic in space. If, in fact, the initial condition is also 2π-periodic in space, then the resulting trajectories converge to a periodic orbit—a traveling wave solution with 4 relative extrema.

Since $\mathcal{A}_{4\pi}$ is connected and contains the traveling wave, the zero solution and the non-zero fixed point, then we know the attractor also contains much more. Figure 2 illustrates points on the global attractor which connect the 2π-periodic traveling wave solution to one of the 4π-periodic fixed points. These points were obtained by taking a limit of symmetry breaking perturbations, in particular, perturbations that are 4π periodic but not 2π periodic. Each horizontal line of the image corresponds to a point in the phase space. Our numerics obtain the same picture, though perhaps shifted in time and space, as we take smaller and smaller perturbations. Upon passing to a subsequence, see Theorem 2.8, we obtain a limit trajectory consisting of wandering non-recurrent points on the global attractor. The focus of this paper is to describe the numerics in detail while providing a rigorous theoretical background.

We emphasize that the traveling wave solution at $t = 0$ appearing at the bottom of the graph has 4 relative extrema and (expect for the perturbation) is recurrent. Similarly, the fixed point when t tends to infinity appearing at the top of the graph has 6 relative extrema, is not 2π-periodic in space and again is recurrent. Although there are set-based algorithms for approximating the global attractor for low-dimensional ordinary differential equations (see, for example, [9]), such techniques are impractical for higher dimensional systems and, in particular, for partial differential equations. However, the main novelty of our research is computing points on the global attractor which are wandering and would never be seen in the limit set resulting from the long-time evolution of any single trajectory.

This paper is organized as follows. Section 2 proves Theorem 2.5, Theorem 2.8 and other analytic results in the specific context of KSE that we will use to support or numerics later on. The theory is, in fact, much more general. We therefore provide a generalization of Theorem 2.5 for a much wider class of dissipative dynamical systems as Theorem 3.8 and Theorem 3.9 in Section 3. Among other dynamical systems, Theorem 3.8 is applicable to the three-dimensional incompressible Navier–Stokes equations while Theorem 3.9 is applicable to the three and two-dimensional incompressible Navier–Stokes equations as well as the Leray-α and LANS-α regularized forms of the Navier–Stokes equations in three-dimensions, see for example, Foias, Holm and Titi [10] and Cheskidov, Holm, Olson and Titi [4] for more information about these turbulence models. Section 4 describes the numerical methods we use, the results of which are presented in Section 5. The paper then finishes with some concluding remarks in Section 6.

2. Theoretical Results

In this section we present the theory needed to support our numerical results. This theory will be generalized in the next section but is presented here in the concrete context of the KSE to build intuition and provide relevance for the more general results later.

The notion of an attractor was first proposed by Liapunov [19] in 1892. In 1955 Coddington and Levinson [5] defined the point attractor as the limits set resulting from the forward evolution of individual trajectories. The global attractor—the

set that attracts the evolution of all bounded sets—was first constructed by Olga Ladyzhenskaya [18] in 1987. Note that the global attractor is a compact connected set which contains the point attractor.

Denote by H_L the space of mean-zero Lebesgue square-integrable L-periodic functions with norm given by

$$\|w\| = \Big(\int_0^L \big|w(x)\big|^2 dx \Big)^{1/2} \qquad \text{for} \qquad w \in H_L. \tag{2.1}$$

We remark that H_L is a Hilbert space and therefore has an inner product. As shown in [6] and [15] the Kuramoto–Sivashinsky equation is well-posed for initial conditions $u_0 \in H_L$ and defines a solution operator S_t such that

$$u(t) = S_t(u_0) \qquad \text{is the solution where} \qquad u(0,x) = u_0(x).$$

For example, solutions with $u_0 \in H_L$ remain bounded in time with respect to the H_L norm.

That said, following Robinson [22], see also [21, 26], we recall

$$\operatorname{dist}(A,B) = \sup_{a\in A} \inf_{b\in B} \|a-b\|,$$

for two sets A and B contained in H_L and

Definition 2.1. The global attractor $\mathcal{A}_L$ is the maximal compact invariant set in H_L such that

$$S_t(\mathcal{A}_L) = \mathcal{A}_L \qquad \text{for all} \qquad t \geq 0$$

and the minimal set that attracts all bounded sets

$$\operatorname{dist}(S_t(X), \mathcal{A}_L) \to 0 \qquad \text{as} \qquad t \to \infty$$

for any bounded set $X \subseteq H_L$.

We further recall that all solutions on the attractor $\mathcal{A}_L$ are uniformly bounded with respect to the H_L norm. In particular, there exists R depending only on μ, ν and L such that for any $u_0 \in H_L$ there is T such that

$$\|u(t)\| \leq R \qquad \text{for all} \qquad t \geq T. \tag{2.2}$$

Estimates for R in terms of μ, ν and L may be found in either [6] or [15].

Our strategy for finding wandering points in $\mathcal{A}_{2L}$ involves applying a perturbation that is $2L$-periodic but not L-periodic to a point in $\mathcal{A}_L$. Before we build up to the theoretical result given in Theorem 2.5, we first discuss some additional properties of the KSE's global attractor. The first result needed is a bound on $|u_x|$ that will be used later in the proof of Lemma 2.6. Although this bound is easy, we present the proof here for completeness and to familiarize the reader with the notations that will be employed in what follows later. Thus, we now state and prove

Theorem 2.2. *There exists a constant R_1 such that*

$$\|u_x(t)\| \leq R_1 \quad \textit{for every} \quad u_0 \in \mathcal{A}_L \quad \textit{and all} \quad t \in \mathbb{R}. \tag{2.3}$$

The proof of Theorem 2.2 follows directly two lemmas which will also be of use in our later analysis. First, we have

Lemma 2.3. *Suppose $\|u(t)\| \leq R$ for all $t \geq T$. There exists M depending only on μ, ν, L and R such that*

$$\int_t^{t+1} \|u_{xx}(s)\|^2 \leq M \qquad \text{for all} \qquad t \geq T.$$

Proof. First, take the H_L inner product of (1.1) with u and integrate by parts to obtain

$$\frac{1}{2}\frac{d}{dt}\|u\|^2 + \int_0^L u^2 u_x dx + \mu \int_0^L u u_{xx} dx + \nu \|u_{xx}\|^2 = 0. \tag{2.4}$$

Now, since

$$\int_0^L u^2 u_x dx = \frac{1}{3}u^3\Big|_0^L = 0$$

and

$$\mu\Big| \int_0^L u u_{xx} dx\Big| \leq \mu \|u\| \|u_{xx}\| \leq \frac{\mu^2}{2\nu}\|u\|^2 + \frac{\nu}{2}\|u_{xx}\|^2,$$

then (2.4) becomes

$$\frac{d}{dt}\|u\|^2 + \nu\|u_{xx}\|^2 \leq \frac{\mu^2}{\nu}\|u\|^2 \leq \frac{\mu^2}{\nu}R^2 \qquad \text{for} \qquad t \geq T.$$

Integrating from t to $t+1$ then yields

$$\|u(t+1)\|^2 + \nu \int_t^{t+1} \|u_{xx}(s)\|^2 \leq \|u(t)\|^2 + \frac{\mu^2}{\nu}R^2 \leq \Big(1 + \frac{\mu^2}{\nu}\Big)R^2$$

So that

$$\int_t^{t+1} \|u_{xx}(s)\|^2 \leq M \qquad \text{where} \qquad M = \Big(1 + \frac{\mu^2}{\nu}\Big)\frac{R^2}{\nu}.$$

This finishes the proof of the lemma. □

The other lemma we state as

Lemma 2.4. *Suppose $\|u(t)\| \leq R$ for all $t \geq T$. There exists R_1 depending only on μ, ν, L and R such that*

$$\|u_x(t)\| \leq R_1 \qquad \text{for all} \qquad t \geq T + 1.$$

Proof. Take the H_L inner product of (1.1) with $-u_{xx}$ and integrate by parts to obtain

$$\frac{1}{2}\frac{d}{dt}\|u_x\|^2 + \nu\|u_{xxx}\|^2 = \mu\|u_{xx}\|^2 + \int_0^L u u_x u_{xx}.$$

Since u has zero average there is $x_0 \in [0, L]$ such that $u(x_0) = 0$. Therefore, by the fundamental theorem of calculus

$$u(\xi) = u(x_0) + \int_{x_0}^{\xi} u_x = \int_{x_0}^{\xi} u_x.$$

Consequently, by the Cauchy–Schwarz inequality

$$\big|u(\xi)\big| = \Big|\int_{x_0}^{\xi} u_x\Big| \leq \int_0^L \big|u_x(x)\big| dx \leq \sqrt{L}\,\|u_x\|$$

and therefore $\|u\|_{L^\infty} \le \sqrt{L}\,\|u_x\|$. Using this bound we estimate

$$\int_0^L u u_x u_{xx} \le \|u\|_{L^\infty} \int_0^L \|u_x u_{xx}\| \le \|u\|_{L^\infty} \|u_x\| \|u_{xx}\| \le \sqrt{L}\,\|u_{xx}\| \|u_x\|^2.$$

It follows that

$$\frac{1}{2}\frac{d}{dt}\|u_x\|^2 + \nu\|u_{xxx}\|^2 \le \mu\|u_{xx}\|^2 + \sqrt{L}\,\|u_{xx}\|\|u_x\|^2. \tag{2.5}$$

Assuming $t-1 \ge T$, choose t_* in the interval $[t-1, t]$ such that $\|u_{xx}\|^2$ is less than its average value. Thus, Lemma 2.3 implies $\|u_{xx}(t_*)\| \le M$. Now, applying the Cauchy–Schwartz inequality yields

$$\|u_x(t_*)\|^2 = -\int_0^L u(t_*, x) u_{xx}(t_*, x)\, dx \le \|u(t_*)\| \|u_{xx}(t_*)\| \le R\sqrt{M}.$$

Consequently, we neglect the term $\|u_{xxx}\|^2$ in (2.5) to obtain

$$\frac{d}{dt}\|u_x\|^2 \le \mu\|u_{xx}\|^2 + \sqrt{L}\,\|u_{xx}\|\|u_x\|^2 \tag{2.6}$$

and then rewrite this as

$$\frac{d}{dt}(\psi\|u_x\|^2) \le \psi\mu\|u_{xx}\|^2 \qquad \text{where} \qquad \psi(t) = \exp\Big(-\sqrt{L}\int_{t_*}^t \big|u_{xx}(s)\big| ds\Big). \tag{2.7}$$

Next, integrating (2.7) over the interval $[t_*, t]$ yields

$$\psi(t)\|u_x(t)\|^2 - \psi(t_*)\|u_x(t_*)\|^2 \le \mu \int_{t_*}^t \psi(s)\|u_{xx}(s)\|^2\, ds$$

and consequently $\psi(t_*) = 1$ implies that

$$\|u_x(t)\|^2 \le \frac{1}{\psi(t)}\|u_x(t_*)\|^2 + \frac{\mu}{\psi(t)}\int_{t_*}^t \psi(s)\|u_{xx}(s)\|^2 ds.$$

Since ψ is a decreasing function and $t_* + 1 > t$, again applying Lemma 2.3 yields

$$\int_{t_*}^t \|u_{xx}\| \le \int_{t_*}^{t_*+1} \|u_{xx}\| \le \sqrt{\int_{t_*}^{t_*+1} \|u_{xx}\|^2} \le \sqrt{M}$$

which then implies

$$\frac{1}{\psi(t)} \le \frac{1}{\psi(t_*+1)} \le e^{\sqrt{LM}}.$$

Upon recalling that $|u_x(t_*)|^2 \le R\sqrt{M}$ we see that

$$\|u_x(t)\|^2 \le e^{\sqrt{LM}}\|u_x(t_*)\|^2 + \mu e^{\sqrt{LM}} \int_{t_*}^{t_*+1} \|u_{xx}(s)\|^2\, ds \le R_1$$

for $t \ge T+1$ where

$$R_1 = (R\sqrt{M} + \mu M)^{1/2} e^{\sqrt{LM}/2}.$$

Noting that R, M and consequently R_1 depend only on L, μ and ν finishes the proof. □

Proof of Theorem 2.2. Since all solutions on the attractor are uniformly bounded with respect to the H_L norm, there is R such that $\|u(t)\| \leq R$ for every $u_0 \in \mathcal{A}_L$ and all $t \in \mathbb{R}$. Noting that Lemma 2.4 holds for any value of T with this value of R finishes the proof. □

With that, we introduce

Theorem 2.5. *Let $\mathcal{A}_L$ be the global attractor of the KSE (1.1) with L-periodic boundary conditions. Given $\epsilon > 0$, there is $\delta > 0$ such that, for any point $v_0 \in L^2([0,L];\mathbb{R})$ with zero average,*

$$\operatorname{dist}(\{v_0\},\mathcal{A}_L) < \delta \qquad \textit{implies} \qquad \operatorname{dist}(\{S_t(v_0)\},\mathcal{A}_L) < \epsilon$$

for all $t \geq 0$.

Before we prove this, we need an estimate on the continuity by which solutions depend on their initial data. Our result is a slight modification of the standard result that compares the evolution of two solutions u and v with different initial conditions u_0 and v_0. In Lemma 2.6 below we further assume $u_0 \in \mathcal{A}_L$ and consequently that $u(t) \in \mathcal{A}_L$ for $t \geq 0$. This additional assumption leads to an estimate with the uniformity needed to later prove Theorem 2.5.

Lemma 2.6. *Let u and v be solutions to the KSE. There is a constant $\beta > 0$ depending only on L, μ and ν such that $u_0 \in \mathcal{A}_L$ and $v_0 \in H_L$ implies*

$$\|u(t) - v(t)\|^2 \leq \|u_0 - v_0\|^2 e^{\beta t} \qquad \textit{for all} \qquad t \geq 0.$$

Proof. Let $w = u - v$ where u and v are both solutions to the KSE. Then

$$\begin{aligned} w_t &= -\nu u_{xxxx} - \mu u_{xx} - u u_x + \nu v_{xxxx} + \mu v_{xx} + v v_x + (u v_x - u v_x) \\ &= -\nu (u-v)_{xxxx} - \mu (u-v)_{xx} - u(u_x - v_x) - v_x (u - v) \\ &= -\nu w_{xxxx} - \mu w_{xx} - u w_x - v_x w + (u_x w - u_x w) \\ &= -\nu w_{xxxx} - \mu w_{xx} - u w_x + w_x w - u_x w. \end{aligned} \tag{2.8}$$

Observe by the L periodicity that

$$\int_0^L w_x w^2 = \frac{1}{3} w^3 \Big|_0^L = 0 \qquad \text{and} \qquad \int_0^L u_x w^2 = -2 \int_0^L u w_x w. \tag{2.9}$$

Therefore, taking the H_L inner product of (2.8) with w and integrating yields

$$\frac{1}{2} \frac{d}{dt} \|w\|^2 + \nu \|w_{xx}\|^2 = \mu \|w_x\|^2 + \int_0^L u w_x w. \tag{2.10}$$

Next, estimate $|u(t,x)|$ pointwise. Since u has zero average by assumption, then for any time t there is a point x_* such that $u(t,x_*) = 0$. Consequently,

$$u(t,x) = u(t,x) - u(t,x_*) = \int_{x_*}^x u_x(t,y)\, dy$$

At this point we use the assumption that $u_0 \in \mathcal{A}_L$ in order to apply (2.3) along with the Cauchy–Schwarz inequality to obtain

$$|u(t,x)| \leq \|u_x\| \sqrt{L} \leq R_1 \sqrt{L} \quad \text{for every} \quad x \in [0,L] \quad \text{and} \quad t \geq 0.$$

Now use this estimate along with Young's inequality, $2ab \leq a^2 + b^2$, to provide a bound on the right-hand side of (2.10):

$$\int_0^L uw_x w \leq \|u\|_{L^\infty}\|w_x\|\|w\| \leq R_1\sqrt{L}\|w_x\|\|w\| \leq \mu\|w_x\|^2 + \frac{R_1^2 L}{4\mu}\|w\|^2.$$

Furthermore, since

$$2\mu\|w_x\|^2 = -2\mu\int_0^L w_{xx}w \leq \|w_{xx}\|\|w\| \leq \nu\|w_{xx}\|^2 + \frac{\mu^2}{\nu}\|w\|^2,$$

then equation (2.10) becomes

$$\frac{d}{dt}\|w\|^2 \leq \beta\|w\|^2 \qquad \text{where} \qquad \beta = \frac{2\mu^2}{\nu} + \frac{R_1^2 L}{2\mu}.$$

We remark that R_1 and consequently β depend only on L, μ and ν. Finally, integrate this differential inequality to obtain the desired result and finish the proof. □

While it is well known that KSE is well-posed (*i.e.*, it has unique solutions which depend continuously on the initial data), the upshot of Lemma 2.6 is that the continuous dependence on initial data is controlled by an explicit constant β which depends only on L, μ and ν. We emphasize that the dependence only on L, μ and ν relies on the fact that one of the solutions lies on the global attractor. We can now prove that if a second solution starts sufficiently close to the attractor, then it will remain close to the attractor for all future times.

Proof of Theorem 2.5. Let $r > 0$ and define

$$X = \bigcup_{u_0 \in \mathcal{A}_L} B_r(u_0) \qquad \text{where} \qquad B_r(u_0) = \left\{\, u \in H_L : \|u - u_0\| < r \,\right\}$$

is the ball of radius r centered at u_0 in H_L. Since $\mathcal{A}_L$ is bounded, then X is bounded. Moreover, X is open and $\mathcal{A}_L \subseteq X$. By Definition 2.1, for all $\epsilon > 0$ there is $T > 0$ such that

$$\operatorname{dist}(S_t(X), \mathcal{A}_L) < \epsilon \qquad \text{for all} \qquad t \geq T. \tag{2.11}$$

Choose $\delta > 0$ sufficiently small such that $\delta < r$ and $\delta^2 e^{\beta T} < \epsilon^2$. Note that since $\delta < r$ then $\operatorname{dist}(\{v_0\}, \mathcal{A}_L) < \delta$ implies $v_0 \in X$. Choose $u_0 \in \mathcal{A}_L$ such that $|u_0 - v_0| < \delta$. It follows that $u(t) = S_t(u_0)$ and $v(t) = S_t(v_0)$ satisfy

$$\|u(t) - v(t)\|^2 \leq \|u_0 - v_0\|^2 e^{\beta t} \leq \delta^2 e^{\beta T} < \epsilon^2 \quad \text{for} \quad t \in [0, T].$$

Consequently,

$$\operatorname{dist}(\{S_t(v_0)\}, \mathcal{A}) < \epsilon \qquad \text{for all} \qquad t \in [0, T].$$

On the other hand, since $v_0 \in X$, we already know from (2.11) that

$$\operatorname{dist}(\{S_t(v_0)\}, \mathcal{A}) < \epsilon \qquad \text{for all} \qquad t > T.$$

Therefore, $\operatorname{dist}(\{S_t(v_0)\}, \mathcal{A}) < \epsilon$ for all $t \geq 0$ which was the desired result. □

For $v_0 \in H_L$ consider the H_L closure of the forward trajectory set

$$W(v_0) = \overline{\{\, S_t(v_0) : t \geq 0 \,\}}. \tag{2.12}$$

We claim that $W(v_0)$ is compact. Since $W(v_0)$ is closed by definition, it is sufficient to show $W(v_0)$ is totally bounded. On other words, for any $\epsilon > 0$ it needs to be shown that $W(v_0)$ can be covered by a finite number of balls of radius ϵ.

Since $\mathcal{A}$ is compact, there is a cover of $\mathcal{A}$ by a finite number of balls $B_{\epsilon/2}(u_n)$ of radius $\epsilon/2$ centered at $u_n \in \mathcal{A}$ where $n = 1, \ldots, N$. Let $U = \cup_{n=1}^{N} B_\epsilon(u_n)$ and note that U is a $\epsilon/2$ neighborhood of $\mathcal{A}$. Thus, there exists T be so large that $S_t(v) \in U$ for all $t \geq T$ and so the set $\{\, S_t(v_0) : t \geq T \,\}$ is covered by a finite number of ϵ balls. Now, since $\{\, S_t(v_0) : 0 \leq 0 \leq T \,\}$ is the continuous image of a compact set $[0, T]$ it is also compact and therefore also covered by a finite number of ϵ balls. It follows that W is totally bounded and hence compact.

Consider the Hausdorff metric $\mathrm{d_H}$ on all compact subsets of H_L defined as

$$\mathrm{d_H}(A, B) = \max(\rho_{\mathrm{H}}(A, B), \rho_{\mathrm{H}}(B, A))$$

where ρ_{H} is the semidistance given by

$$\rho_{\mathrm{H}}(A, B) = \sup_{u_1 \in A} \inf_{u_2 \in B} \|u_1 - u_2\|.$$

It is known $\mathrm{d_H}$ is a compact metric space provided the original metric space is compact, but, of course, H_L is not compact. We therefore consider the weaker space V_L^* defined as the dual of $V_L = \{v \in H_L : \|v_x\| \leq \infty\}$ with respect to the H_L inner product. Note the norm on V_L^* is given by

$$\|u\|_* = \sup \Big\{ \textstyle\int_0^L uv \quad : \quad v \in V_L \quad \text{and} \quad \|v_x\| \leq 1 \Big\}.$$

Since the closed r-ball $\overline{B_r(0)} = \big\{\, u \in H_L : \|u\| \leq r \,\big\}$ is compact in the topology of V_L^*, then for any $\epsilon > 0$ the space of all compact subsets of $\overline{B_{R+\epsilon}(0)}$ is a compact space with respect to the weak Hausdorff metric $\mathrm{d}_{\mathrm{H}}^*$ given by the semidistance

$$\rho_{\mathrm{H}}^*(A, B) = \sup_{u_1 \in A} \inf_{u_2 \in B} \|u_1 - u_2\|_*.$$

Lemma 2.7. *Let $u_0 \in \mathcal{A}_L$ and $v_n \in H_L$ be such that $\|u_0 - v_n\| \to 0$. Then there is a subsequence n_j such that the forward trajectory sets $W(v_{n_j})$ form a Cauchy sequence with respect to $\mathrm{d}_{\mathrm{H}}^*$ metric.*

Proof. Given $\epsilon > 0$, Theorem 2.5 implies there is $\delta > 0$ such that

$$\|u_0 - v_n\| < \delta \qquad \text{implies} \qquad \operatorname{dist}(\{S_t(v_n)\}, \mathcal{A}_L) \leq \epsilon$$

for all $t \geq 0$. Consequently, there is N large enough such that

$$W(v_n) \subseteq \overline{B_{R+\epsilon}(0)} \qquad \text{for all} \qquad n \geq N.$$

Since the space of all compact subsets of $\overline{B_{R+\epsilon}}$ is compact with respect to the weak Hausdorff metric $\mathrm{d}_{\mathrm{H}}^*$, then there is a subsequence n_j such that $W(v_{n_j})$ is Cauchy. □

Since every compact metric space is complete, it immediately follows from Lemma 2.7 that there exists a compact set $K \in \overline{B_{R+\epsilon}(0)}$ such that

$$\mathrm{d}_{\mathrm{H}}^*(K, W(v_{n_j})) \to 0 \qquad \text{as} \qquad j \to \infty.$$

In accordance with the terminology used in the introduction when outlining the computational steps for finding wandering points, we shall call K a limit trajectory of the perturbations of u_0. Before finishing this section, we note that the convergence of $W(v_{n_j})$ to K also occurs with respect to the norm in H_L. In particular, we have

Theorem 2.8. *Let n_j be the subsequence from Lemma 2.7. Then*

$$\mathrm{d_H}(K, W(v_{n_j})) \to 0 \qquad as \qquad j \to \infty.$$

Proof. To simplify the notation—relabeling if necessary—we assume without loss of generality that $\mathrm{d^*_H}(K, W(v_n)) \to 0$ as $n \to \infty$. Upon choosing N so large that $W(v_n) \subseteq \overline{B_{R+\epsilon}(0)}$ for all $n \geq N$ it follows that $v(t) = S_t(v_n)$ satisfies $\|v(t)\| \leq R+\epsilon$ for all $t \geq 0$. Lemma 2.4 then implies there exists an R_1 depending only on μ, ν, L and $R + \epsilon$ such that

$$\|v_x(t)\| \leq R_1 \qquad \text{for all} \qquad t \geq 1.$$

Let $\epsilon_n > 0$ be a sequence monotonically decreasing to zero such that

$$\|u_0 - v_n\| \leq \epsilon_n \qquad \text{and} \qquad \mathrm{d^*_H}(K, W(v_n)) \leq \epsilon_n \qquad \text{for all} \qquad n \in \mathbb{N}.$$

Suppose $m \geq k$ and $n \geq k$ where $k \geq N$ and set $u(t) = S_t(u_0)$ and $w(t) = S_t(v_m)$. Since

$$\rho^*_{\mathrm{H}}(W(v_n), W(v_m)) \leq \epsilon_n + \epsilon_m \leq 2\epsilon_k,$$

then for any $s \geq 0$ there is $t \geq 0$ such that $\|v(s) - w(t)\|_* \leq 3\epsilon_k$. We now consider four cases depending on whether s and t are bigger or smaller than one.

If $s \geq 1$ and $t \geq 1$, we obtain by interpolation that

$$\|v(s) - w(t)\| \leq \|v_x(s) - w_x(t)\|^{1/2} \|v(s) - w(t)\|_*^{1/2} \leq (2R_1)^{1/2}(3\epsilon_k)^{1/2}.$$

If $s \geq 1$ and $t < 1$, we obtain by Lemma 2.6 that

$$\begin{aligned} \|v(s) - w(t)\| &\leq \|v(s) - u(t)\| + \|u(t) - w(t)\| \\ &\leq \|v_x(s) - u_x(t)\|^{1/2} \|v(s) - u(t)\|_*^{1/2} + \|u_0 - v_m\| e^{\beta t/2} \\ &\leq (2R_1)^{1/2}(3\epsilon_k)^{1/2} + \epsilon_k e^{\beta/2}. \end{aligned}$$

If $s < 1$ and $t \geq 1$, the estimate is similar and again

$$\|v(s) - w(t)\| \leq (2R_1)^{1/2}(3\epsilon_k)^{1/2} + \epsilon_k e^{\beta/2}.$$

If both $s \leq 1$ and $t \leq 1$, then

$$\begin{aligned} \|v(s) - w(t)\| &\leq \|v(s) - u(s)\| + \|u(s) - u(t)\| + \|u(t) - w(t)\| \\ &\leq \|v_n - u_0\| e^{\beta s/2} + (2R_1)^{1/2} \|u(s) - u(t)\|_*^{1/2} + \|w_n - u_0\| e^{\beta t/2} \\ &\leq 2\epsilon_k e^{\beta/2} + (2R_1)^{1/2} \|u(s) - u(t)\|_*^{1/2} \end{aligned}$$

and since

$$\begin{aligned} \|u(s) - u(t)\|_* &\leq \|u(s) - v(s)\|_* + \|v(s) - w(t)\|_* + \|w(t) - u(t)\|_* \\ &\leq \|v_n - u_0\| e^{\beta s/2} + \|v(s) - w(t)\|_* + \|v_m - u_0\| e^{\beta t/2} \\ &\leq 2\epsilon_k e^{\beta/2} + 3\epsilon_k \end{aligned}$$

it follows that

$$\|v(s) - w(t)\| \leq 2\epsilon_k e^{\beta/2} + (2R_1)^{1/2}(2\epsilon_k e^{\beta/2} + 3\epsilon_k).$$

In light of the fact that the bounds on $\|v(s) - w(t)\|$ tend to zero as $k \to \infty$ in each of the cases, we conclude that $W(v_n)$ is Cauchy with respect to Hausdorff metric $\mathrm{d_H}$ on compact sets in H_L. As the only thing it could converge to is again K, the result follows. □

When all the perturbations v_n break a symmetry of u_0, this theoretical result is of practical use for computing wandering points on the attractor. For example, in the numerical computations which follow we take

$$v_n = u_0 + \delta \cdot \text{single Fourier mode that breaks the symmetry.}$$

In that case K connects u_0 to a part of the attractor in which the symmetry of u_0 has been broken, moreover, if the symmetry never spontaneously returns, then there are points in K that must be wandering.

Before turning to those computations we first note that the above theoretical framework is, in fact, much more general than the analysis just worked out for the Kuramoto–Sivashinsky equations in this section.

3. General Theory

Theorem 2.5 can be extended to the general context of dissipative dynamical systems which we now do. We state first some definitions and results that will be needed in the general development and then proceed the perturbation of initial conditions on the attractor.

3.1. **Preliminaries.** We recall the definition of the *evolutionary system* introduced in [2]. Let $(X, \mathrm{dist_s}(\cdot,\cdot))$ be a metric space endowed with a metric $\mathrm{dist_s}$, which will be referred to as a strong metric. Let $\mathrm{dist_w}(\cdot,\cdot)$ be another metric on X satisfying the following conditions:

(1) X is $\mathrm{dist_w}$-compact.
(2) If $\mathrm{dist_s}(u_n, v_n) \to 0$ as $n \to \infty$ for some $u_n, v_n \in X$, then $\mathrm{dist_w}(u_n, v_n) \to 0$ as $n \to \infty$.

Due to the property 2, $\mathrm{dist_w}(\cdot,\cdot)$ will be referred to as a weak metric on X.

In applications we usually we choose X to be an absorbing ball and define the strong and weak distances by

$$\mathrm{dist_s}(u,v) = \|u - v\|_{L^2} \qquad \text{and} \qquad \mathrm{dist_w}(u,v) = \|u - v\|_{H^{-\ell}} \quad \text{where} \quad \ell > 0.$$

Note the Rellich–Kondrachov theorem implies $H^{-\ell}$ is compactly embedded into L^2.

Denote by $\overline{A}^{\bullet}$ the closure of a set $A \subset X$ in the topology generated by $\mathrm{d}_\bullet$ where $\bullet = \mathrm{s}$ or w represents either the strong or weak topologies. Note that any strongly compact ($\mathrm{dist_s}$-compact) set is weakly compact ($\mathrm{dist_w}$-compact) and any weakly closed set is strongly closed.

Let $C([a,b]; X_\bullet)$, where $\bullet = \mathrm{s}$ or w, be the space of $\mathrm{d}_\bullet$-continuous X-valued functions on $[a,b]$ endowed with the metric

$$d_{C([a,b];X_\bullet)}(u,v) = \sup_{t\in[a,b]} \mathrm{d}_\bullet(u(t), v(t)).$$

Let also $C([a,\infty);X_\bullet)$ be the space of $\mathrm{d}_\bullet$-continuous X-valued functions on $[a,\infty)$ endowed with the metric

$$d_{C([a,\infty);X_\bullet)}(u,v)=\sum_{T\in\mathbb{N}}\frac{1}{2^T}\frac{\sup\{\mathrm{d}_\bullet(u(t),v(t)):a\le t\le a+T\}}{1+\sup\{\mathrm{d}_\bullet(u(t),v(t)):a\le t\le a+T\}}.$$

To define the evolutionary system, first let

$$\mathcal{T}=\{\,I\quad:\quad I=[T,\infty)\subset\mathbb{R}\quad\text{or}\quad I=(-\infty,\infty)\,\},$$

and for each $I\subset\mathcal{T}$, let $\mathcal{F}(I)$ denote the set of all X-valued functions on I.

Definition 3.1. A map $\mathcal{E}$ that associates to each $I\in\mathcal{T}$ a subset $\mathcal{E}(I)\subset\mathcal{F}$ will be called an evolutionary system if the following conditions are satisfied:

(1) $\mathcal{E}([0,\infty))\neq\emptyset$.
(2) $\mathcal{E}(I+s)=\big\{\,u(\cdot):u(\cdot+s)\in\mathcal{E}(I)\,\big\}$ for all $s\in\mathbb{R}$.
(3) $\big\{\,u(\cdot)|_{I_2}:u(\cdot)\in\mathcal{E}(I_1)\,\big\}\subset\mathcal{E}(I_2)$ for all pairs $I_1,I_2\in\mathcal{T}$ such that $I_2\subset I_1$.
(4) $\mathcal{E}((-\infty,\infty))=\big\{\,u(\cdot):u(\cdot)|_{[T,\infty)}\in\mathcal{E}([T,\infty))$ for every $T\in\mathbb{R}\,\big\}$.

We will refer to $\mathcal{E}(I)$ as the set of all trajectories on the time interval I. Trajectories in $\mathcal{E}((-\infty,\infty))$ will be called complete. Let $P(X)$ be the set of all subsets of X. For every $t\ge0$, define a map $R(t)\colon P(X)\to P(X)$ by

$$R(t)A=\big\{\,u(t):u\in A,u(\cdot)\in\mathcal{E}([0,\infty))\,\big\}\qquad\text{where}\qquad A\subset X.$$

Note that the assumptions on $\mathcal{E}$ imply that $R(s)$ enjoys the following property:

$$R(t+s)A\subset R(t)R(s)A\quad\text{for every}\quad A\subset X\quad\text{and}\quad t,s\ge0. \tag{3.1}$$

Definition 3.2. The $\omega_\bullet$-*limit* ($\bullet=\mathrm{s},\mathrm{w}$) of a set $A\subset X$ is

$$\omega_\bullet(A):=\bigcap_{T\ge0}\overline{\bigcup_{t\ge T}R(t)A}^{\,\bullet}.$$

We also note that an equivalent definition of the $\omega_\bullet$-limit set is given by

$$\omega_\bullet(A)=\Big\{x\in X:\ \begin{array}{c}\text{there exist } t_n\to\infty \text{ and } x_n\in R(t_n)A\\ \text{such that } x_n\to x \text{ in the } \mathrm{d}_\bullet\text{-metric}\end{array}\Big\}.$$

Finally, we will give a precise definition of the global attractor.

Definition 3.3. A set $A\subset X$ is a $\mathrm{d}_\bullet$-*attracting set*, if it uniformly attracts X in $\mathrm{d}_\bullet$-metric, *i.e.*, for any ε there exits t_0 such that

$$\mathrm{dist}_\bullet(\{x\},A)=\inf_{a\in\mathcal{A}}d_\bullet(x,a)<\varepsilon\quad\text{for every}\quad x\in R(t)X\quad\text{and}\quad t\ge t_0.$$

A set $\mathcal{A}_\bullet\subset X$ is a $\mathrm{d}_\bullet$-*global attractor* if $\mathcal{A}_\bullet$ is a minimal $\mathrm{d}_\bullet$-closed $\mathrm{d}_\bullet$-attracting set.

Evolutionary systems $\mathcal{E}$ whose trajectories are solutions to the KSE, or even the three-dimensional incompressible Navier–Stokes equations, also satisfy the following properties:

A1 $\mathcal{E}([0,\infty))$ is a compact set in $C([0,\infty);X_\mathrm{w})$.

A2 (Energy inequality) Assume that X is a set in some Banach space H satisfying the Radon-Riesz property with the norm denoted by $\|\cdot\|$, so that $\mathrm{dist_s}(x,y) = \|x-y\|$ for $x, y \in X$ and $\mathrm{dist_w}$ induces the weak topology on X. Assume also that for any $\epsilon > 0$, there exists δ, such that for every $u \in \mathcal{E}([0,\infty))$ and $t > 0$,

$$\|u(t)\| \le \|u(t_0)\| + \epsilon,$$

for t_0 a.e. in $(t-\delta, t) \cap [0,\infty)$.

A3 (Strong convergence a.e.) Let $u, u_n \in \mathcal{E}([0,\infty))$ be such that $u_n \to u \in \mathcal{E}([0,\infty))$ in $C([0,T]; X_\mathrm{w})$ for some $T > 0$. Then $u_n(t) \to u(t)$ strongly a.e. in $[0,T]$.

Definition 3.4. A Banach space H with the norm $\|\cdot\|$ satisfies the Radon-Riesz property if $x_n \to x$ in H if and only if $x_n \to x$ weakly and $\lim \|x_n\| = \|x\|$ as $n \to \infty$.

The following results were proved in [2,3]:

Theorem 3.5. *If $\mathcal{A}_\bullet$ exists, then $\mathcal{A}_\bullet = \omega_\bullet(X)$.*

Theorem 3.6. *Let $\mathcal{E}$ be an evolutionary system satisfying A1. Then the weak global attractor $\mathcal{A}_\mathrm{w}$ exists and*

$$\mathcal{A}_\mathrm{w} = \big\{\, u_0 : u_0 = u(0) \text{ for some } u \in \mathcal{E}((-\infty,\infty)) \,\big\}.$$

Furthermore, if $\mathcal{E}$ also satisfies A2, A3 and every complete trajectory is strongly continuous, then

(1) *The strong global attractor $\mathcal{A}_\mathrm{s}$ exists, it is strongly compact and $\mathcal{A}_\mathrm{s} = \mathcal{A}_\mathrm{w}$.*
(2) *(Strong uniform tracking property) For any $\epsilon > 0$ and $T > 0$ there exists t_0 such that for any $t^* > t_0$ every trajectory $u \in \mathcal{E}([0,\infty))$ satisfies $\mathrm{dist_s}(u(t), v(t)) < \epsilon$ for all $t \in [t^*, t^*+T]$ for some complete trajectory $v \in \mathcal{E}((-\infty,\infty))$.*

3.2. **Perturbations of Initial Conditions.**

Definition 3.7. A set $A \in X$ is positively invariant if

$$R(t)A \subset A \qquad \text{for every} \qquad t \ge 0.$$

The global attractor $\mathcal{A}_\mathrm{w}$ is often positively invariant in applications. Indeed, due to Theorem 3.6, $\mathcal{A}_\mathrm{w}$ is positively invariant if the following concatenation property holds: *For every $u_1 \in \mathcal{E}((-\infty,\infty))$ and $u_2 \in \mathcal{E}([0,\infty))$ with $u_1(0) = u_2(0)$, then $v \in \mathcal{E}((-\infty,\infty))$, where v is the "glued" trajectory*

$$v(t) = \begin{cases} u_1(t) & \text{for} \quad t < 0, \\ u_2(t) & \text{for} \quad t \ge 0. \end{cases}$$

We are now ready to prove a weak version of Theorem 2.5 stated as

Theorem 3.8. *Let $\mathcal{E}$ be an evolutionary system satisfying A1 and let $\mathcal{A}_\mathrm{w}$ be the weak global attractor of $\mathcal{E}$. Assume that $\mathcal{A}_\mathrm{w}$ is positively invariant. Then given $\epsilon > 0$ there is $\delta > 0$ such that for every trajectory $u \in \mathcal{E}([0,\infty))$ then*

$$\mathrm{dist_w}(\{u(0)\}, \mathcal{A}_\mathrm{w}) < \delta \qquad \textit{implies} \qquad \mathrm{dist_w}(\{u(t)\}, \mathcal{A}_\mathrm{w}) < \epsilon$$

for all $t \geq 0$.

Proof. Assume to the contrary that there exist $\epsilon > 0$ and a sequence $u_n \in \mathcal{E}([0,\infty))$ such that $\mathrm{dist}_{\mathrm{w}}(\{u_n(0)\}, \mathcal{A}_{\mathrm{w}}) < 1/n$, but

$$\mathrm{dist}_{\mathrm{w}}(\{u_n(t_n)\}, \mathcal{A}_{\mathrm{w}}) \geq \epsilon \tag{3.2}$$

for some sequence $t_n \geq 0$. First, consider the case where $\{t_n\}$ is bounded, *i.e.*, there exists T such that $t_n \leq T$ for all n. Since $\mathcal{E}([0,\infty))$ is a compact set in $C([0,\infty); X_{\mathrm{w}})$ due to A1, there is $u \in C([0,\infty); X_{\mathrm{w}})$ and a subsequence n_j such that $u_{n_j} \to u$ in $C([0,\infty); X_{\mathrm{w}})$ as $j \to \infty$. Hence, there exists J such that

$$\mathrm{dist}_{\mathrm{w}}(u_{n_j}(t), u(t)) < \epsilon \tag{3.3}$$

for all $j \geq J$ and $t \in [0,T]$. Since $\mathrm{dist}_{\mathrm{w}}(u_n(0), \mathcal{A}_{\mathrm{w}}) < 1/n$, it follows that $u(0) \in \mathcal{A}_{\mathrm{w}}$. Finally, since $\mathcal{A}_{\mathrm{w}}$ is positively invariant, we have that $u(t) \in \mathcal{A}_{\mathrm{w}}$ for all $t \geq 0$. Thus, thanks to (3.3) $\mathrm{dist}_{\mathrm{w}}(u_{n_j}(t), \mathcal{A}_{\mathrm{w}}) < \epsilon$ for all $j \geq J$ and $t \in [0,T]$, contradicting (3.2).

Now consider the remaining case where $\{t_n\}$ is unbounded. Then we can pass to a subsequence and drop a subindex to have $t_n \to \infty$ as $n \to \infty$. Since X is $\mathrm{dist}_{\mathrm{w}}$-compact, there is $x \in X$ such that passing to another subsequence and dropping a subindex gives

$$\mathrm{dist}_{\mathrm{w}}(u_n(t_n), x) \to 0 \qquad \text{as} \qquad n \to \infty. \tag{3.4}$$

By definition of ω-limit,

$$x \in \omega_{\mathrm{w}}(X).$$

Therefore, Theorem 3.5 implies that $x \in \mathcal{A}_{\mathrm{w}}$. Then (3.4) yields $\mathrm{dist}_{\mathrm{w}}(u_n(t_n), \mathcal{A}_{\mathrm{w}}) \to 0$ as $n \to \infty$, contradicting (3.2). □

While the above theorem applies to the 3D Navier-Stokes equations, there are numerous examples, such as the KSE considered in this paper, that induce asymptotically $\mathrm{dist}_{\mathrm{s}}$-compact evolutionary systems and hence possess strong global attractors $\mathcal{A}_{\mathrm{s}}$. Such evolutionary systems usually emerge from subcritical equations enjoying some regularity properties and hence satisfying the following condition.

A4 (Uniform strong convergence) Let $u_n \in \mathcal{E}([0,\infty))$ be such that $u_n \to u$ in $C([0,T]; X_{\mathrm{w}})$ for some $u \in \mathcal{E}([0,\infty))$ and $T > 0$. If $\mathrm{dist}_{\mathrm{s}}(u_n(0), u(0)) \to 0$ as $n \to \infty$, then $\mathrm{dist}_{\mathrm{s}}(u_n(t), u(t)) \to 0$ uniformly on $[0,T]$.

For such evolutionary systems we can prove the following.

Theorem 3.9. *Let $\mathcal{E}$ be an evolutionary system satisfying A1 and A4. Assume also that $\mathcal{E}$ possesses a strongly compact positively invariant strong global attractor $\mathcal{A}_{\mathrm{s}}$. Then given $\epsilon > 0$, there is $\delta > 0$, such that for every trajectory $u \in \mathcal{E}([0,\infty))$ then*

$$\mathrm{dist}_{\mathrm{s}}(\{u(0)\}, \mathcal{A}_{\mathrm{s}}) < \delta \qquad \textit{implies} \qquad \mathrm{dist}_{\mathrm{s}}(\{u(t)\}, \mathcal{A}_{\mathrm{s}}) < \epsilon$$

for all $t \geq 0$.

Proof. Assume to the contrary that there exist $\epsilon > 0$ and a sequence $u_n \in \mathcal{E}([0,\infty))$ such that $\mathrm{dist}_{\mathrm{s}}(\{u_n(0)\}, \mathcal{A}_{\mathrm{s}}) < 1/n$, but

$$\mathrm{dist}_{\mathrm{s}}(u_n(t_n), \mathcal{A}_{\mathrm{s}}) \geq \epsilon \tag{3.5}$$

for some $t_n \geq 0$. First, consider the case where $\{t_n\}$ is bounded, *i.e.*, there exists T such that $t_n \leq T$ for all n. Note that there exists a sequence $a_n \in \mathcal{A}_{\mathrm{s}}$ such that $\mathrm{dist}_{\mathrm{s}}(u_n(0), a_n) < 1/n$. Since $\mathcal{A}_{\mathrm{s}}$ is strongly compact, there exists $a \in \mathcal{A}_{\mathrm{s}}$, such that after passing to a subsequence and dropping a subindex we have $a_n \to a$ and, consequently, $u_n(0) \to a$ strongly as $n \to \infty$.

Now since $\mathcal{E}([0,\infty))$ is a compact set in $C([0,\infty); X_{\mathrm{w}})$ due to A1, there are $u \in C([0,\infty); X_{\mathrm{w}})$ and a subsequence n_j such that $u_{n_j} \to u$ in $C([0,\infty); X_{\mathrm{w}})$ as $j \to \infty$. Clearly $u(0) = a$ and $u_{n_j}(0) \to u(0)$ strongly as $n \to \infty$. Thanks to A4, $\mathrm{dist}_{\mathrm{s}}(u_{n_j}(t), u(t)) \to 0$ as $j \to \infty$ uniformly on $[0,T]$. Hence, there exists J such that

$$\mathrm{dist}_{\mathrm{s}}(u_{n_j}(t), u(t)) < \epsilon \tag{3.6}$$

for all $j \geq J$ and $t \in [0,T]$. Recall that $u(0) = a \in \mathcal{A}_{\mathrm{s}}$. Since $\mathcal{A}_{\mathrm{s}}$ is positively invariant, we have that $u(t) \in \mathcal{A}_{\mathrm{s}}$ for all $t \geq 0$. Thus, thanks to (3.6), for every $t \in [0,T]$, we have $\mathrm{dist}_{\mathrm{s}}(u_{n_j}(t), \mathcal{A}_{\mathrm{s}}) < \epsilon$ for all $j \geq J$ and $t \in [0,T]$, contradicting (3.5).

Now consider the remaining case where $\{t_n\}$ is unbounded. Then we can pass to a subsequence and drop a subindex to have $t_n \to \infty$ as $n \to \infty$. Since X is $\mathrm{dist}_{\mathrm{s}}$-compact, there is $x \in X$ such that passing to another subsequence and dropping a subindex gives

$$\mathrm{dist}_{\mathrm{s}}(u_n(t_n), x) \to 0 \qquad \text{as} \qquad n \to \infty. \tag{3.7}$$

By definition of ω-limit,

$$x \in \omega_{\mathrm{s}}(X).$$

Therefore, Theorem 3.5 implies that $x \in \mathcal{A}_{\mathrm{s}}$. Then (3.7) yields $\mathrm{dist}_{\mathrm{s}}(u_n(t_n), \mathcal{A}_{\mathrm{s}}) \to 0$ as $n \to \infty$, contradicting (3.5). □

As an end to this section, we note the proof of Lemma 2.7 was already based on general properties of compactness and so carries directly over to the general setting. We further leave the extension of Theorem 2.8 to the reader.

4. Numerical Methods

In order to present our computational results, we first describe the numerical schemes used for our calculations. We employed three different numeric schemes, not only to approximate solutions or to study their evolution over time, but also to confirm the correctness of our results. One scheme was a first-order method used for preliminary calculations and to verify the correctness of a higher order method used for our final results. For our final results we used a refinement of the Cox–Matthews method (see also Zavalani [27] for particular details relating to the KSE) described by Kassam and Trefethen in [16]. This method is a numerical regularization of the fourth-order method derived and proposed by Cox and Matthews [8] to avoid loss of precision. We remark that the computational work for this paper also provides an independent verification that without such regularization the original Cox–Matthews scheme is unsuitable for approximating solutions to the KSE.

All computations were performed using a Fourier series representation of the solutions. In particular, we use fast Fourier transforms to approximate

$$u(t,x) \approx \sum_{k=-M/2+1}^{M/2} \hat{u}_k(t) e^{ikx} \tag{4.1}$$

and the nonlinear term as

$$u(t,x)u_x(t,x) \approx \sum_{k=-M/2+1}^{M/2} \hat{\mathcal{B}}_k(u(t,\cdot)) e^{ikx},$$

where $\hat{\mathcal{B}}_k$ are defined as the Fourier coefficients of the function $x \mapsto u(x)u_x(x)$.

Our first-order method is a split time-stepping method where the linear terms are integrated exactly in time and the nonlinear term is integrated according to an explicit Euler time step. Specifically, we set $t_n = t_0 + nh$ where $h > 0$ and compute

$$\hat{u}_k^{n+1} = \begin{cases} (\hat{u}_k^n - h\mathcal{B}_k)\exp(h(\mu|k|^2 - \nu|k|^4)) & \text{for } k \in [-M/2, M/2] \\ 0 & \text{otherwise.} \end{cases}$$

MATLAB code to implement this scheme appears in Appendix B of [24]. Note that the code forces the solution $u(t,x)$ to be real valued by taking the real part of every inverse fast Fourier transform performed throughout the code. This turns out to be necessary: without it, rounding error leads to a nonzero imaginary part that exponentially grows and eventually destroys the approximation. Note that we also enforce the fact that our solution $u(t,x)$ has zero average by setting $\hat{u}_0 = 0$ at every time step. Note the required periodicity of the solution is enforced automatically by working in the Fourier representation.

The fourth-order method employed in our computations is the Runge–Kutta method derived by Cox and Matthews [8] and refined by Kassam and Trefethen [16]. The Cox–Matthews fourth-order method is

$$\begin{aligned} \hat{u}_k^{n+1} = {} & \hat{u}_k^n e^{ch} + \{F(\hat{u}_k^n, t_n)[-4 - ch + e^{ch}(4 - 3hc + h^2c^2)] \\ & + 2(F(a_n, t_n + h/2) + F(b_n, t_n + h/2))[2 + ch + e^{ch}(hc - 2)] \\ & + F(c_n, t_n + h)[-4 - 3ch - h^2c^2 + e^{ch}(4 - ch)]\}/h^2c^3. \end{aligned}$$

where

$$\begin{aligned} a_n &= \hat{u}_k^n e^{ch/2} + \left(e^{ch/2} - 1\right) F(\hat{u}_k^n, t_n)/c, \\ b_n &= \hat{u}_k^n e^{ch/2} + \left(e^{ch/2} - 1\right) F(a_n, t_n + h/2)/c, \\ c_n &= a_n e^{ch/2} + \left(e^{ch/2} - 1\right) \left(2F(b_n, t_n + h/2) - F(\hat{u}_k^n, t_n)\right)/c. \end{aligned}$$

For the KSE, the constant $c = \mu|k|^2 - \nu|k|^4$ depends on k, and $F(u,t) = -\mathcal{B}_k(u)$. MATLAB code to implement the original Cox–Matthews's method was created for comparison purposes and also appears Appendix B of [24]. A modification of Cox and Matthews's fourth-order method was described by Kassam and Trefethen [16] to avoid loss of precision when computing the coefficients $-4 - ch + e^{ch}(4 - 3hc + h^2c^2)$, $2 + ch + e^{ch}(hc - 2)$, $-4 - 3ch - h^2c^2 + e^{ch}(4 - ch)$ and $e^{ch/2} - 1$. The MATLAB code

to implement this method appearing in Kassam and Trefethen [16] was adapted for our final computations.

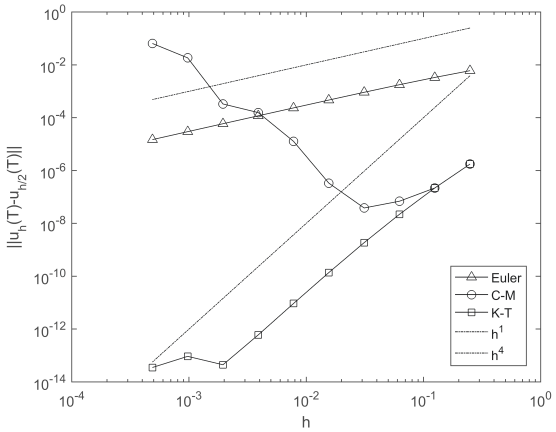

FIGURE 3. A convergence study of the original Cox–Matthews fourth-order exponential time integrator compared to the version modified by Kassam–Trefethen to avoid loss of precision in the context of the KSE when $\mu = 0.1$, $\nu = 0.027$, $L = 2\pi$ and $T = 1.0$. For reference the first-order exponential Euler method is also depicted.

Figure 3 compares the rate of convergence of the Euler, Cox–Matthews and Kassam–Trefethen methods when computing the traveling wave or periodic orbit depicted by Figure 6 for the KSE when $\mu = 0.1$, $\nu = 0.027$ and $L = 2\pi$. This test demonstrates the original Cox–Matthews method suffers from loss of precision so severe the theoretical fourth-order convergence is barely evident. The Kassam–Trefethen modification, on the other hand, has the same accuracy for large values of h as the Cox–Matthews method and maintains the fourth-order convergence to achieve error levels below 10^{-9}.

4.1. **Rescaling.** The numerical methods discussed in the previous section each approximate 2π-periodic solutions where u is given by (4.1). In order to compute solutions on a 4π-periodic domain, we rescale μ, ν and L using a factor λ as follows.

Given an L-periodic solution $u(x + L, t) = u(x, t)$ for all $x \in \mathbb{R}$ we first rescale x by the scaling factor λ. Taking $\xi = \lambda x$ allows us to view u as an $L\lambda$-periodic function of ξ. Then $d\xi/dx = \lambda$ and

$$u_x = \frac{\partial u}{\partial x} = \frac{\partial u}{\partial \xi}\frac{d\xi}{dx} = \lambda u_\xi.$$

Similarly, $u_{xx} = \lambda^2 u_{\xi\xi}$ and $u_{xxxx} = \lambda^4 u_{\xi\xi\xi\xi}$. Then the KSE given by (1.1) becomes

$$u_t + \lambda u u_\xi + \mu\lambda^2 u_{\xi\xi} + \nu\lambda^4 u_{\xi\xi\xi\xi} = 0.$$

Next, we rescale t. Let $\tau = \eta t$. We get $u_t = \eta u_\tau$, yielding

$$\eta u_\tau + \lambda u u_\xi + \mu\lambda^2 u_{\xi\xi} + \nu\lambda^4 u_{\xi\xi\xi\xi} = 0. \tag{4.2}$$

By setting $\eta = \lambda$, we can divide both sides by λ to obtain

$$u_\tau + uu_\xi + \mu\lambda u_{\xi\xi} + \nu\lambda^3 u_{\xi\xi\xi\xi} = 0.$$

Thus, we transform the equation (1.1) with L-periodic boundary conditions using the parameters

$$\xi = \lambda x, \qquad \tau = \lambda t, \qquad \tilde{\mu} = \mu\lambda, \qquad \tilde{\nu} = \nu\lambda^3$$

to obtain

$$u_\tau + uu_\xi + \tilde{\mu}u_\xi + \tilde{\nu}u_{\xi\xi\xi\xi} = 0,$$

which has the $L\lambda$-periodic boundary conditions needed for our computational experiments.

5. Computational Results

Theorem 2.5 as well as the more general Theorem 3.8 or Theorem 3.9 each show that if the perturbation is small, then the resulting trajectory remains close to the attractor for all future times. When considering the trajectories of solutions which arise from such perturbations, it will be useful to define the L-periodicity measure for $w \in H_{2L}$ to be

$$p(w) = \Big(\int_0^{2L} \big|w(x) - w(x+L)\big|^2 dx \Big)^{1/2}. \tag{5.1}$$

Note that $w \in \mathcal{A}_L$ implies $p(w) = 0$; however, $p(w) > 0$ for any point $w \in \mathcal{A}_{2L} \setminus \mathcal{A}_L$.

For the choice of parameters $L = 2\pi$, $\mu = 0.1$ and $\nu = 0.027$, the numerics in this section suggest that vanishingly small perturbations which are $2L$ periodic but not L periodic break the symmetry in a way which never returns as $t \to \infty$. Once the symmetry is broken, the solution eventually converges to a fixed point with L-periodicity measure $p(u) \approx 1.6193$, see equation (5.1). Moreover, the trajectories in phase space taken by the symmetry-breaking perturbations converge—subject to a translation in x—to a unique set of points as the size of the perturbation vanishes. In particular, Theorem 2.8 implies there is a subsequence that accounts for the translations in x axis and for which the resulting trajectories converge in the Hausdorff metric to points on the global attractor.

5.1. **A Fixed Point and a Traveling Wave.**

For our first set of calculations we used the following parameters: $L = 4\pi$, $\mu = 0.1$ and $\nu = 0.027$. These computations were performed using the fourth-order exponential time integrator described in the previous section with fast Fourier transforms of size $M = 1024$ and a time step of size $h = 1/100$. Note that in order to compute a 4π-periodic solution using our numeric codes we rescaled the equation by setting $\tilde{\mu} = 0.05$ and $\tilde{\nu} = 0.003375$ as in (4.2). It was observed when starting with a number of different initial conditions that the solution converged to a fixed point consisting of three relative maxima and three relative minima. Figure 4 depicts this 4π-periodic fixed point solution. Other initial conditions converged to the same curve translated in space.

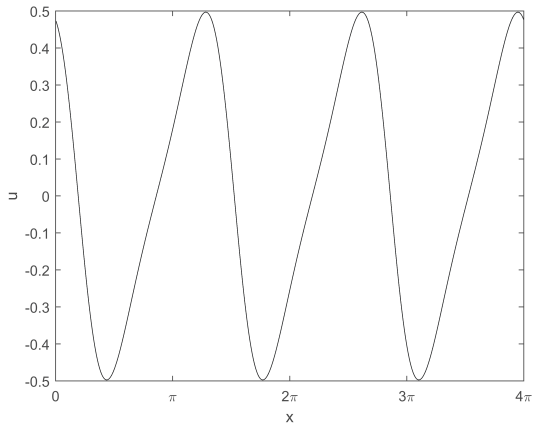

FIGURE 4. The fixed point with $\|u\| \approx 1.1804$ obtained after a long-time computational run when $\mu = 0.1$, $\nu = 0.027$ and $L = 4\pi$.

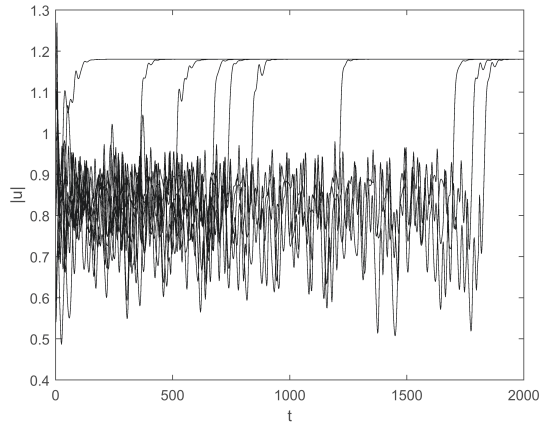

FIGURE 5. Evolution of $\|u(t)\|$ starting at 10 different randomly chosen 4π-periodic initial conditions. Each trajectory converges to a fixed point with norm approximately equal to 1.1804.

In particular, random initial conditions were sampled from the probability distribution

$$u_0(x) = \sum_{k=-M/2+1}^{M/2} \delta Z_k e^{-\gamma|k|} e^{ik\xi} \qquad \text{with} \qquad \xi = x/2, \tag{5.2}$$

where

$$Z_k = \begin{cases} X_k \exp(2\pi i Y_k) & \text{for } k > 0, \\ 0 & \text{for } k = 0, \\ X_{-k} \exp(-2\pi i Y_{-k}) & \text{for } k < 0, \end{cases}$$

and X_k and Y_k were uniform independent random variables on the interval $[0, 1]$. Here $\delta \approx 287.2777$ and $\gamma = 0.2$ were chosen so that

$$\mathbf{E}\big[\|u_0\|\big] \approx 1 \qquad \text{and} \qquad e^{-\gamma N/2} \approx 10^{-23}.$$

Thus, the expected norm of the initial condition is similar in magnitude to the norm of the subsequent evolution of the solution and the amplitudes of the highest Fourier modes are essentially zero in comparison to the lowest ones. The exponential decay of the Fourier modes given by the parameter γ further ensures theoretically that the initial condition is smooth in space as $M \to \infty$. Note also that $Z_{-k} = \overline{Z_k}$ implies the initial condition is real-valued and $Z_0 = 0$ implies the mean is zero.

For each of the random initial conditions chosen according to (5.2), the resulting trajectories converged to a spatial translation of the fixed point depicted in Figure 4. The evolution of the norm for trajectories corresponding to ten representative 4π-periodic initial conditions appear in Figure 5. We remark that the time it took for each of the different trajectories to reach the fixed point varied greatly. Note that the norm traces leading immediately preceding the the appearance of the fixed point, though arguably close to the attractor, are different for each trajectory. Hence there is no obvious way to determine how close to the attractor those points really are. We also note that it is possible to make a simple spatial translation of each initial condition without changing the dynamics so the resulting trajectories all end at the exact same fixed point. Finally, these computations were repeated using the Euler and original Cox–Matthews schemes and the same fixed point found in each case.

Since, any of the initial conditions considered above could be translated in space by varying amounts, it follows that all translations of the fixed point appearing in Figure 4 must be contained in the global attractor $\mathcal{A}_{4\pi}$. Therefore, we let $\mathcal{L}$ be the subset of phase space which contains all translates of that fixed point and note that the global attractor $\mathcal{A}_{4\pi}$ contains $\mathcal{L}$. Because the zero solution is also a fixed point, we know that $0 \in \mathcal{A}_{4\pi}$. It follows that $\{0\} \cup \mathcal{L} \subset \mathcal{A}_{4\pi}$. Now, since the global attractor is a connected set, this means there must be additional points in the attractor that connect 0 to $\mathcal{L}$. Thus, the attractor is much more complicated than the fixed points that have been exhibited so far. We shall now use the theory presented in sections 2 and 3 of this paper to compute some of the additional points in $A_{4\pi}$ by means of symmetry-breaking perturbations.

While we could, at this point, perturb the origin as illustrated in the simple example (1.2) appearing in the introduction to find a connecting trajectory from the origin to the fixed point in Figure 4, there is much more complexity to the attractor of the KSE than that. Since the fixed point in Figure 4 is not 2π-periodic, we now consider specially chosen initial conditions in the 4π-periodic domain which are, in fact, 2π-periodic. Since the KSE preserves periodicity, no matter how far forward in time any 2π-periodic initial condition is evolved, it will never converge to the fixed point in Figure 4. We therefore repeat a similar numerical experiment as before, except this time starting with randomly chosen initial conditions that are 2π-periodic in space.

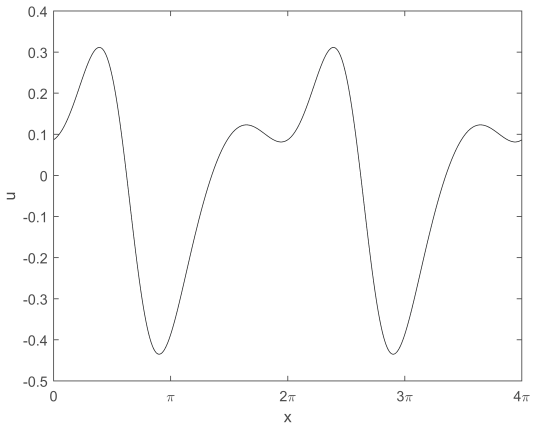

FIGURE 6. A 2π-periodic traveling wave with $\|u\| = 0.7794$ obtained when $\mu = 0.1$, $\nu = 0.027$ and $L = 2\pi$.

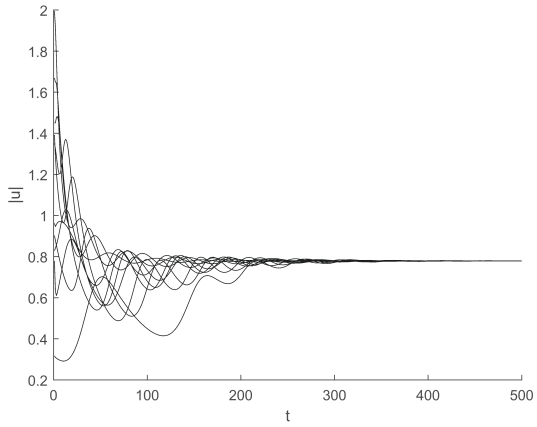

FIGURE 7. Evolution of $\|u(t)\|$ starting at 10 different randomly chosen 2π-periodic initial conditions. Each trajectory converges to a traveling wave with norm approximately equal to 0.7794 and velocity ± 0.0724.

When $L = 2\pi$ the resulting trajectories converged to a periodic oribit or traveling wave solution consisting of two relative maxima and two relative minima. Sometimes the wave moved from right to left and other times the result was a mirror image which moved from left to right. The speed of the traveling wave was approximately 0.0724, or equivalently, the period of the orbit in phase space was 86.78 units of time. Figure 6 depicts the version of the traveling wave solution that moved from right to left. The evolution of the norm for trajectories corresponding to ten representative 2π-periodic initial conditions appear in Figure 7. Note that these initial conditions converge much sooner to the periodic orbit than the analogous trajectories in Figure 5 did for the $L = 4\pi$ case. As before, the norm traces leading

immediately preceding the the appearance of the traveling wave, though arguably close to the attractor, are different for each trajectory.

Let $\mathcal{M}$ be the subset of phase space which contains the function depicted in Figure 6, its translates, and the mirror images of its translates. We conclude that global attractor $\mathcal{A}_{2\pi}$ contains $\mathcal{M}$. Moreover, since $\mathcal{A}_{2\pi} \subseteq \mathcal{A}_{4\pi}$ then

$$\{0\} \cup \mathcal{L} \cup \mathcal{M} \subseteq \mathcal{A}_{4\pi}.$$

It is worth remarking that one could also consider a π-periodic initial condition. Although the π-periodicity is preserved as the initial condition is evolved forward in time, the resulting solution converges to zero as $t \to \infty$. Since the zero solution is π-periodic (as well as periodic with respect to any other period) there is no contradiction here. However, no new points on the $\mathcal{A}_{4\pi}$ periodic attractor are found in this case.

One more case remains to be considered: the case of the $4\pi/3$-periodic initial condition. However, initial conditions which are $4\pi/3$-periodic again converge to the same fixed point described in Figure 4, and no new points on the global attractor have been found.

The next section uses symmetry breaking to compute wandering points on the global attractor that connect the $\mathcal{L}$ with $\mathcal{M}$.

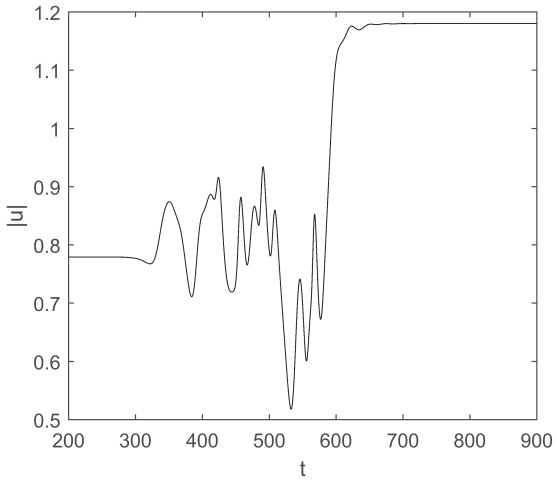

FIGURE 8. The evolution of $\|u(t)\|$ for a trajectory with initial condition given by the 2π-periodic traveling wave plus a 4π-periodic perturbation that is not 2π-periodic.

5.2. **Breaking the Symmetry.** Let $u_{\text{traveling}}(t, x)$ represent the 2π-periodic traveling wave depicted in Figure 6 and consider the perturbation

$$u_\delta(x) = (2\pi)^{-1/2}\delta \cos(x/2)$$

where $\delta = 10^{-8}$. Note that u_δ is 4π-periodic but not 2π-periodic and that $\|u_\delta\| = \delta$. Figure 8 illustrates the time evolution of $\|u(t)\|$ for the trajectory $u(t)$ with initial

condition

$$u_0(x) = u_{\text{traveling}}(0, x) + u_\delta(x).$$

We remark that $\|u(t)\| \approx 0.7794$ for $t < 270$. After this the perturbation becomes noticeable and $\|u(t)\|$ fluctuates and hits its lowest level around $t \approx 535$ before converging to approximately $\|u(t)\| \approx 1.1804$ for $t > 700$.

Theorem 2.5 implies that if δ is small enough, then $u(t)$ will stay close to $\mathcal{A}_{4\pi}$ for all $t > 0$. Even though $u(0, x)$ is within 10^{-8} of the 2π-periodic traveling wave and $u(700, x)$ is similarly close to the 4π-periodic fixed point, further evidence is needed before concluding that $u(t, x)$ is close to $\mathcal{A}_{4\pi}$ for every $t \in [0, T]$. To verify that δ is small enough, we try different sizes of δ and look, as provided by Theorem 2.8, for convergence along a subsequence.

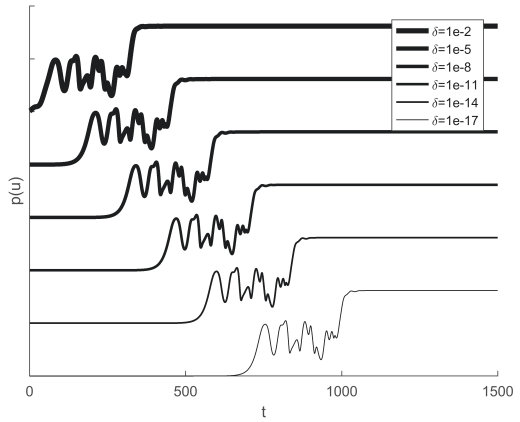

FIGURE 9. Evolution of the periodicity measure $p(u)$ over time. Trajectories for different values of δ have been vertically offset for clarity. Smaller values of δ shift the graph to the right with $u(t)$ tracing a similar trajectory through phase space.

When δ is smaller it takes longer for the effects of the perturbation to make a noticeable difference on the symmetry of the resulting solution. To measure the time it takes to fully break the symmetry we monitor the L-periodicity measure $p(u)$ given in (5.1) with $L = 2\pi$. Figure 9 details the results of such monitoring for value of δ ranging through fifteen decimal orders of magnitude from 10^{-2} to 10^{-17}. Observe that the 2π-periodicity measure starts at near zero and goes through the same oscillating pattern for each value of δ tested before leveling off to the non-zero measure of the 4π-periodic fixed point depicted in Figure 4. The presence of such a distinct pattern and the fact that the L-periodicity measure p is translation invariant suggests the subsequences of Theorem 2.8 will be easy to find numerically and need only take translations of the x axis into account.

To determine the relative position of the pattern we define

$$T_\delta = \sup\big\{\, T : p(u(t)) \le 0.1 \text{ for all } t \in [0, T] \,\big\}.$$

Thus T_δ is the last time the periodicity measure of the 2π periodicity of the solution u falls below 0.1 and beyond which the solution is never even approximately 2π

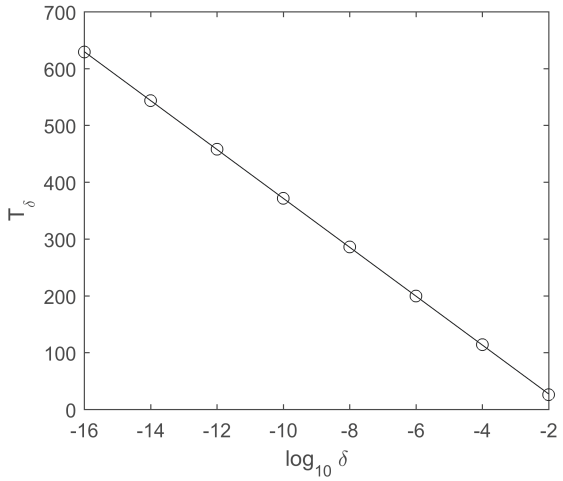

FIGURE 10. Graph of T_δ versus δ where T_δ is the time needed for the 2π-symmetry to be broken by a δ-sized perturbation.

periodic in space. Note that 0.01, 1.5 or any other value that uniquely determines the relative position of the oscillating pattern in Figure 9 for different values of δ would work equally well.

Figure 10 plots the values of T_δ versus $\log_{10}(\delta)$ for $\delta = 10^{-n}$ for $n \in \{2, 4, \ldots, 16\}$. The points lie in a straight line given by the least squares fit

$$T_\delta \approx -43.043 \log_{10}(\delta) - 58.486.$$

The visual quality of the fit is striking: Changing δ changes the symmetry-breaking time by an easily predictable amount over a range of 14 orders of magnitude. In particular, while smaller values of δ appear to delay when the symmetry is broken, the pattern with which the symmetry is broken is essentially the same in all cases.

Representative trajectories are depicted in Figure 11 for $\delta = 10^{-2}$ and 10^{-12}. Both trajectories have been shifted in time to take into account the different values T_δ. Note after adjusting for T_δ and the translation in x, each graph appears very similar as the one given earlier in Figure 2. Thus, our numerics suggest there exists x_δ such that the sequence of initial conditions given by

$$v_n(x) = u_{\text{traveling}}(0, x - x_\delta) + u_\delta(x - x_\delta) \qquad \text{where} \qquad \delta = 10^{-n}$$

and the forward trajectory sets $W(v_n)$ defined in (2.12) converge to a limit trajectory $\mathcal{K}$ in the Hausdorff metric From a visual point of view, the set $\mathcal{K}$, is indestinguishable from the trajectory depicted in Figure 2. Moreover, all of the points in $\mathcal{K}$ with the exception of those also in $\mathcal{L}$ and $\mathcal{M}$ are wandering.

6. Conclusion

The goal of this paper was to use symmetry-breaking perturbations to find wandering points on the global attractor of the KSE which are nonrecurrent. To support our computational results we have developed rigorous mathematical analysis concerning purturbations of points on the attractor and the convergence of the resulting

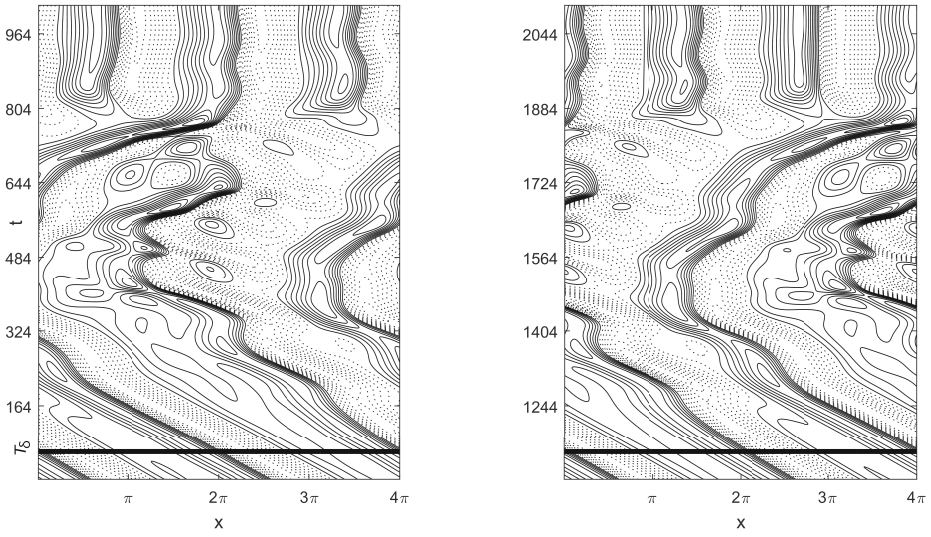

FIGURE 11. Different values of δ lead to similar graphs translated in x. The graph on the left represents the points for $\delta = 10^{-2}$ and the right for $\delta = 10^{-12}$.

forward trajectory sets $W(v_n)$ in the Hausdorff metric to a limit trajectory $\mathcal{K}$ which lies on the global attractor. This theory was worked out in details for the KSE and then presented in a generalized way that applies to many other dissipative dynamical systems, including a weak form suitable for the three-dimensional Navier–Stokes equations. Numerically a visualization of $\mathcal{K}$ for a specific choice of parameters in the KSE was computed and appears in this paper as Figure 2.

Numerically, our results are approximations good to within the resolution of the spatial Fourier discretization, the truncation error in fourth-order exponential time integrator and the double-precision arithmetic used for our computations. For example, numerical rounding implies that

$$\text{float}((2\pi)^{-1/2}\delta\cos(x/2) + u_0(x)) = \text{float}(u_0(x)) \tag{6.1}$$

whenever δ is 15 orders of magnitude smaller than $u_0(x)$. Since $u_0(x) \neq 0$ over most of the domain, making such a perturbation in the physical space would severely limit the precision of our computations. On the other hand, the same perturbation (up to a phase shift) may be written in Fourier space as

$$\frac{\delta}{\sqrt{8\pi}} + \hat{u}_1 \qquad \text{and} \qquad \frac{\delta}{\sqrt{8\pi}} + \hat{u}_{-1}$$

where $\hat{u}_k$ are the Fourier modes of u_0. Since u_0 is 2π periodic, it follows that $\hat{u}_k = 0$ for all k odd. Therefore, the rounding issues which appear in the physical space do not appear when the Fourier modes are perturbed by any representable nonzero δ.

On the other hand, the nonlinear term uu_x is always computed in the physical space by means of fast Fourier transforms. Therefore, even if it is possible to represent the perturbation of u_0 in Fourier space accurately for very small values

of δ, the resulting nonlinear terms used in our numerics are still subject to the rounding issue already mentioned in (6.1). A numerical check of the non-linear term suggests that higher precision floating-point arithmetic would be needed for values of δ smaller than 10^{-19}.

We end by noting that, while our numerics are supported by the mathematical theory developed in sections 2 and 3, the simulations themselves are approximate in nature and do not leverage any additional analytic and topological properties to guarantee, for example, that the KSE really does posses a fixed point similar to Figure 4 or a periodic orbit similar to Figure 2. Therefore, while the evidence is compelling, we have not provided a rigorous numerical proof that the points we found are wandering or even on the attractor. Such rigor is, unfortunately, outside the scope of the present work. At the same time the rigorous numerics of [1] and [11] mentioned in the introduction for the KSE suggest that such results may also be possible for the present computation. The authors feel future work that extends the technique developed here along such lines would be extremely interesting.

References

[1] G. Arioli and H. Koch, *Computer-assisted methods for the study of stationary solutions in dissipative systems, applied to the Kuramoto-Sivashinski equation*, Arch. Ration. Mech. Anal. **197** (2010), 1033–1051.

[2] A. Cheskidov and C. Foias, On global attractors of the 3D Navier-Stokes equations, Journal of Differential Equations **231** (2006), 714–754.

[3] A. Cheskidov, *Global attractors of evolutionary systems*, Journal of Dynamics and Differential Equations **21** (2009), 249–268.

[4] A. Cheskidov, D. D. Holm, E. Olson and E.S. Titi, *On a Leray-alpha model of turbulence*, Proc. R. Soc Long. Ser. A Math. Phys. Eng. Sci. **461** (2005), 629–649.

[5] E. Coddington and N. Levinson, *Theory of Ordinary Differential Equations*, McGraw–Hill, 1955.

[6] P. Collet, J. P. Eckmann, H. Epstein and J. Stubbe, *A global attracting set for the Kuramoto–Sivashinsky equation* Communications in Mathematical Physics **152**, 203–214, 1993.

[7] R. Conte and M. Musette, *Painlevé analysis and Bäcklund transformation in the Kuramoto-Sivashinsky equation*, Journal of Physics A **22** (1989), 169–177.

[8] S. M. Cox and P. C. Matthews, *Exponential time differencing for stiff systems*, Journal of Computational Physics URL `www.sciencedirect.com/science/article/pii/S0021999102969950`, August 2001, 430–455,.

[9] M. Dellnitz and O. Junge, *On the approximation of complicated dynamical behavior*, SIAM J. Numer. Anal. **36** (1999), 491–515.

[10] C. Foias, D. D. Holm and E.S. Titi, *The three dimensional viscous Camassa–Holm equations and their relation to the Navier–Stokes equations and turbulence theory*, Journal of Dynamics and Differential Equations **14** (2002), 1–35.

[11] J. Figueras and R. de la Llave, *Numerical computations and computer assisted proofs of periodic orbits of the Kuramoto-Sivashinsky equation*, SIAM J. Appl. Dyn. Syst. **16** (2017), 834–852.

[12] G. W. Griffiths and W. E. Schiesser, *Traveling Wave Analysis of Partial Differential Equations: Numerical and Analytical Methods with Matlab and Maple*, Academic Press, 2012.

[13] Z. Grujić, *k Spatial Analyticity on the Global Attractor for the Kuramoto–Sivashinsky Equation*, Journal of Dynamics and Differential Equations **12** (2000), 217–228.

[14] G. M. Homsy, *Model equations for wavy viscous film flow*, Lectures in Applied Mathematics, **15** (1974), 191–201.

[15] Ju. S. Il'yashenko, *Global Aaalysis of the phase portrait for then Kuramoto–Sivashinsky equation*, Journal of Dynamics and Differential Equations **4** (1992), 585–615.

[16] A. K. Kassam and L. N. Trefethen, *Fourth-order time stepping for stiff PDEs*, SIAM Journal on Scientific Computing **26** (2005), 1214–1233.
[17] Y. Kuramoto and T. Suzuki, *Persistent propagation of concentration waves in dissipative media far from thermal equilibrium*, t Progr. Theoret. Phys. **55** (1976), 356–359.
[18] O. A. Ladyzhenskaya, *On finding the minimal global attractors for the Navier–Stokes equations and other PDEs*, Russian Mathematical Surveys **42** (1987), 27–73.
[19] A. M. Liapunov, *The general problem of the stability of motion*, *Kharkov Mathematical Society* (1982), 1–250.
[20] A. A. Nepomnyashchii, *Stability of wavy conditions in a film flowing down an inclined plane*, Fluid Dynamics **9** (1975), 354–359.
[21] B. Nicolaenko, B. Scheurer and R. Temam, *Some global dynamical properties of the Kuramoto–Sivashinsky equation: Nonlinear stability and attractors*, Physica D **16** (1985), 155–183.
[22] J. C. Robinson, *Infinite-Dimensional Dynamical Systems: An Introduction to Dissipative Parabolic PDEs and the Theory of Global Attractors*, Cambridge University Press, 2001.
[23] G. Sivashinsky, *Nonlinear analysis of hydrodynamic instability in laminar flames, Part I. Derivation of basic equations*, Acta Astronautica **4** (1977), 1177–1206.
[24] B. Smith, *Symmetry-breaking perturbations on the global attractor of the Kuramoto–Sivashinsky equation*, Masters Thesis, University of Nevada, Department of Mathematics and Statistics, 2017.
[25] E. Tadmor, *The well-posedness of the Kuramoto-Sivashinsky equation*, SIAM Journal on Mathematical Analysis **17** (1986), 884–893.`https://ntrs.nasa.gov/archive/nasa/casi.ntrs.nasa.gov/19840024982.pdf`
[26] R. Temam, *Infinite-Dimensional Dynamical Systems in Mechanics and Physics*, Second Edition. Springer, 1997.
[27] G. Zavalani, *Fourier spectral methods for numerical solving of the Kuramoto-Sivashinsky equation*, American Journal of Numerical Analysis **2** (2014), 90–97.

Manuscript received
revised

A. Cheskidov
Department of Mathematics, University of Illinois at Chicago, Chicago, IL 60607, USA
E-mail address: `acheskid@uic.edu`

E. Olson
Department of Mathematics and Statistics, University of Nevada, Reno, NV 89557, USA
E-mail address: `ejolson@unr.edu`

B. Smith
Department of Mathematics and Statistics, University of Nevada, Reno, NV 89557, USA
E-mail address: `beaus@nevada.unr.edu`